

EPR, Electronic Spectra, and Electron Transfer Properties of the 17 Electron Carbonylhydrotris(triphenylphosphine)rhodium(II) Cation

Dmitri Menglet,[†] Alan M. Bond,^{*,†} Kevin Coutinho,[†] Ron S. Dickson,[†] Georgii G. Lazarev,[†] Scott A. Olsen,[†] and John R. Pilbrow[‡]

Contribution from the Departments of Chemistry and Physics, Monash University, Clayton, Victoria 3168, Australia

Received September 9, 1997

Abstract: An unusually stable five-coordinate monomeric divalent rhodium complex, $[\text{Rh}^{\text{II}}(\text{H})(\text{CO})(\text{PPh}_3)_3]^+$, is produced by bulk oxidative electrolysis or chemical oxidation of $\text{Rh}^{\text{I}}(\text{H})(\text{CO})(\text{PPh}_3)_3$ in dichloromethane. Consequently, odd as well as even electronic configurations are available in this well-known catalytic system. The EPR and electronic spectra of electrogenerated paramagnetic 17-electron cation $[\text{Rh}^{\text{II}}(\text{H})(\text{CO})(\text{PPh}_3)_3]^+$ have been obtained at low temperatures as has the EPR spectrum of the deuterated analogue. Computer simulation of the EPR spectra of the hydride and deuteride complexes reveals three *g*-values and anisotropic coupling constants for hydrogen, phosphorus, and rhodium. One of the phosphorus coupling constants is very large ($A_1 = 175.0 \text{ G}$; $A_2 = 176.0 \text{ G}$; $A_3 = 230.0 \text{ G}$). This may be accounted for if $[\text{Rh}^{\text{II}}(\text{H})(\text{CO})(\text{PPh}_3)_3]^+$ has the square pyramidal structure, and substantial mixing of the singly occupied metal orbital and the apical phosphorus *s*-orbital are considered. NMR measurements on mixtures of $\text{Rh}^{\text{I}}(\text{H})(\text{CO})(\text{PPh}_3)_3$ and $[\text{Rh}^{\text{II}}(\text{H})(\text{CO})(\text{PPh}_3)_3]^+$ are consistent with a very fast electron self-exchange reaction and the heterogeneous charge-transfer rate constant for the $[\text{Rh}^{\text{II}}(\text{H})(\text{CO})(\text{PPh}_3)_3]^+/0$ redox couple also is very fast. One electron electrochemical oxidation of $[\text{Rh}^{\text{I}}(\text{H})(\text{CO})(\text{PPh}_3)_3]^+$ to $[\text{Rh}^{\text{III}}(\text{H})(\text{CO})(\text{PPh}_3)_3]^{2+}$ is followed by a very fast reductive elimination reaction (loss of proton) which generates $[\text{Rh}^{\text{I}}(\text{CO})(\text{PPh}_3)_3]^+$.

Introduction

The 18 electron $\text{Rh}^{\text{I}}(\text{H})(\text{CO})(\text{PPh}_3)_3$ complex is one of the most commercially important homogeneous catalysts.^{1,2} Consequently, the chemistry of this rhodium(I) compound has been widely investigated in order to understand mechanisms associated with its reactivity. Of particular importance has been the dissociation of the triphenylphosphine to generate a 16 electron $\text{Rh}^{\text{I}}(\text{H})(\text{CO})(\text{PPh}_3)_2$ moiety.^{3,4}

An electrochemical study of the oxidation of the $\text{Rh}(\text{H})(\text{CO})(\text{PPh}_3)_3$ complex in acetonitrile was published in 1977.^{5,6} The data revealed that a reversible one electron oxidation process was available on the voltammetric time scale and that further oxidation also was possible. However, no spectroscopic evidence for existence of the presumed 17 electron monomeric $[\text{Rh}(\text{H})(\text{CO})(\text{PPh}_3)_3]^+$ species, containing the uncommon divalent rhodium(II) oxidation state, was presented, nor were details of the products of the second process characterized. In this paper we wish to report the results of an electrochemical and

spectroscopic study in dichloromethane which provides direct evidence that a moderately stable, but rare, monomeric 17 electron Rh(II) compound is in fact formed by bulk electrolysis of the important Rh(I) catalyst. The product of the second one-electron process also is identified and other features associated with electron-transfer reactions in this well-known catalytic system also are established in this investigation.

Experimental Section

$\text{Rh}(\text{H})(\text{CO})(\text{PPh}_3)_3$ was prepared as described in the literature.⁷ The deuterated sample used for electrooxidation and EPR measurements was prepared in situ in both CH_2Cl_2 and CD_2Cl_2 solution by H–D exchange³ using deuterium gas (Matheson). The completion of the exchange reaction was confirmed by IR spectroscopy.^{3,8} The oxidized form was prepared (but not isolated) by slow addition of a CH_2Cl_2 solution containing equivalent amount of ferrocenium hexafluorophosphate to the CH_2Cl_2 solution of the Rh(I) complex under nitrogen gas. $[\text{Rh}^{\text{I}}(\text{CO})(\text{PPh}_3)_3]\text{BF}_4$ was synthesized according to the literature procedure.⁹

Electrochemical measurements and electrosynthesis was carried out in 0.2 M $[\text{Bu}^n_4\text{N}]\text{BF}_4$ solution in CH_2Cl_2 . The electrolyte, $[\text{Bu}^n_4\text{N}]\text{BF}_4$, was prepared by neutralizing aqueous $[\text{Bu}^n_4\text{N}]\text{OH}$ (Aldrich) with HBF_4 (Aldrich). The product was washed by warm deionized water and subsequently recrystallized three times from methanol/water (4:1) and dried in vacuo for 4 h. HPLC purity grade CH_2Cl_2 (Mallinckrodt) was used for the electrochemical measurements. Dichloromethane used for the spectroelectrochemical experiments was predried over KOH pellets before distilling from CaH_2 immediately prior to an electrochemical experiment. Cyclic (CV) and rotating disk voltammetry

[†] Department of Chemistry.

[‡] Department of Physics.

(1) Jardine, F. H. *Polyhedron* 1982, 1, 569–605.

(2) Dickson, R. S. *Homogeneous Catalysis with Compounds of Rhodium and Iridium*; D. Reidel Publishing Company, Dordrecht, 1985. Parshall, G. W.; Iteel, S. D. *Homogeneous Catalysis: the Applications and Chemistry of Catalysis by Soluble Transition Metal Complexes*, 2nd ed.; John Wiley & Sons: New York, 1992.

(3) Evans, D.; Yagupsky, G.; Wilkinson, G. *J. Chem. Soc. (A)* 1968, 2660–2665.

(4) Brown, J. M.; Canning, L. R.; Kent, A. G.; Sidebottom, P. J. *J. Chem. Soc., Chem. Commun.* 1982, 721–723.

(5) Valcher, S.; Pilloni, G.; Martelli, M. *J. Electroanal. Chem.* 1973, 42, App.5–App.6.

(6) Pilloni, G.; Schiavon, G.; Zotti, G.; Zecchin, S. *J. Organomet. Chem.* 1977, 134, 305–318.

(7) Ahmad, N.; Levison, J. J.; Robinson, S. D.; Uttley, M. F. *Inorg. Synth.* 1974, 15, 59–60.

(8) Vaska, L. *J. Am. Chem. Soc.* 1966, 88, 4100–4101.

(9) Legzdins, P.; Mitchel, R. W.; Rempel, G. L.; Fuddick, J. D.; Wilkinson, G. *J. Chem. Soc. (A)* 1970, 3322–3326.

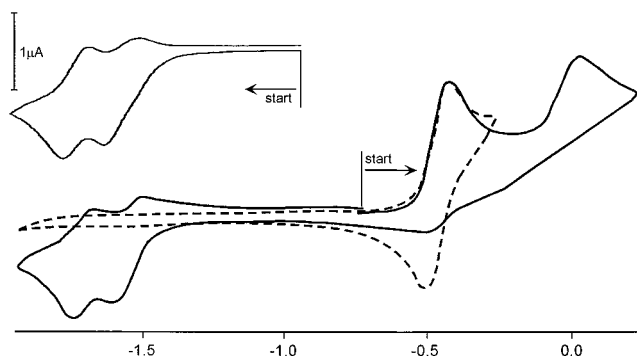


Figure 1. Cyclic voltammograms of 1×10^{-3} M $\text{Rh}^{\text{I}}(\text{H})(\text{CO})(\text{PPh}_3)_3$ using a platinum macrodisk electrode in a dichloromethane solution at 298 K. Insert is a voltammogram for the reduction of 1×10^{-3} M of $[\text{Rh}^{\text{I}}(\text{CO})(\text{PPh}_3)_3]^+$ which verifies that this is the product of the second process for oxidation of $[\text{Rh}^{\text{I}}(\text{H})(\text{CO})(\text{PPh}_3)_3]^+$.

measurements at platinum macrodisk working Pt auxiliary and Ag/AgCl reference electrodes were carried out using a BAS-100 Electrochemical Analyzer or a Cypress System (CYSY-1R). A Metrohm 628-10 assembly was used for rotating disk electrode experiments. The potential of this electrode was calibrated against that of the reversible Fc/Fc^+ redox couple (Fc = ferrocene) from voltammetric data obtained from the oxidation of 5×10^{-4} M ferrocene in dichloromethane (0.1 M $[\text{Bu}^n_4\text{N}]\text{BF}_4$). The electrolyte solutions were purged with nitrogen gas, and the cell was constantly maintained under an inert atmosphere.

Bulk electrolysis was performed using a two-compartment cell, with a platinum mesh basket working electrode, a double-fritted Ag/AgCl reference electrode, and the second platinum mesh basket counter electrode separated from the bulk solution by a glass frit. Dry ice/acetone bath was used to achieve low temperatures (ca. 210 K).

Electronic spectra were recorded using a Perkin-Elmer $\lambda 9$ double-beam UV/vis/near-IR spectrophotometer with digital background subtraction capability. The spectra of electrogenerated species were collected in situ, by the use of an *optically transparent thin layer-electrochemical* (OTTLE) quartz cell, with a fine platinum minigrad as working electrode (ca. 70% transmittance), mounted within the sample compartment of the spectrophotometer. The cell placed in the reference beam was of similar profile and contained a matching section of platinum minigrad. The deoxygenated sample solution was prepared and transferred via syringe into the sample cell. The working, auxiliary, and reference electrodes were added to the sample cell and connected to a Thompson E-series Ministat potentiostat. During an experiment the cells (sample and reference) were cryostatted in gastight, double-glazed PTFE cell blocks, enabling both the cells and their contents to be cooled by cold N_2 gas. The N_2 gas was chilled by passing it through a copper coil immersed in liquid nitrogen. The electrolysis was continued until the spectrum ceased to change and the current decayed to a constant minimum. After completion, the potential was reset and the spectrum of the starting complex regenerated.

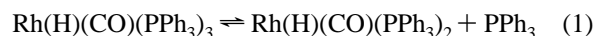
X-band EPR spectra of frozen solution (glass) in CH_2Cl_2 containing 0.2 M $[\text{Bu}^n_4\text{N}]\text{BF}_4$ electrolyte were recorded in deoxygenated EPR tubes at 77 K, using Bruker ESP-300 E and Varian E-12 spectrometers.

^1H NMR experiments on samples of partially electrolyzed solution were obtained at 20 °C using a Bruker DRX 400 (MHz) spectrometer. Chemical shifts are referenced against tetramethylsilane.

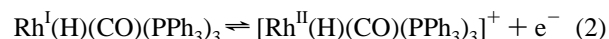
Results and Discussion

Electrochemistry and Electronic Spectroscopy. Cyclic voltammograms of the $\text{Rh}(\text{H})(\text{CO})(\text{PPh}_3)_3$ complex at a platinum disk electrode over the scan rate range of 50–2000 mV s^{-1} at room temperature in the presence of 0.2 M $[\text{Bu}^n_4\text{N}]\text{BF}_4$ as the electrolyte in dichloromethane solution reveal the presence of a chemically and electrochemically reversible oxidation process (Figure 1) which has a reversible potential of -0.48 V vs Fc/Fc^+ as calculated from the average of the oxidation and reduction peak potentials. Thus, a plot of peak height versus

the square root of scan rate was linear, and the peak-to-peak separation of the oxidation and reduction peak potentials was identical to those for the known reversible oxidation of ferrocene for which the heterogeneous charge-transfer rate constant¹⁰ is $\geq 1 \text{ cm s}^{-1}$ and therefore reversible under conditions used for the cyclic voltammetric experiments. Voltammograms for the first oxidation process in dichloromethane are consistent with literature data reported in acetonitrile.^{5,6} Importantly, the voltammetry is unaffected by the presence of up to a 5-fold concentration excess of triphenylphosphine in the solution. In the thermodynamic sense, this result implies that the equilibrium position for the reaction

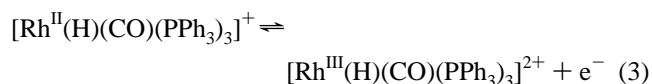


and the analogous reaction for the oxidized form of the compound must lie a long way to the left in dichloromethane. The initial oxidation process therefore can be assigned to the chemically and electrochemically reversible reaction



Rotating disk voltammetry confirms that the first oxidation process is diffusion controlled, since the limiting current (i_L) is linearly dependent on the square root of rotation rate (rotation rate 500–3000 rpm). Additionally, a plot of E vs $\ln[(i_L - i)/i_L]$ is linear with a slope of RT/F at 20 °C at all rotation rates examined. The reversible half wave potential is -0.48 V vs Fc/Fc^+ which is identical to the value obtained from cyclic voltammetry.

A second chemically irreversible one electron oxidation process (Figure 1) is observed at about 0 V vs Fc/Fc^+ under both cyclic voltammetric and rotating disk electrode conditions. On the reverse scan, two reversible processes are observed at -1.57 and -1.74 V vs Fc/Fc^+ (Figure 1). These two processes are identical to those observed when voltammetric reduction of the compound $[\text{Rh}^{\text{I}}(\text{CO})(\text{PPh}_3)_3]^+$ is studied (Figure 1). This process is therefore readily shown to be of the EC type, in which the $\text{Rh}(\text{II}/\text{III})$ oxidation step is followed by rapid reductive elimination of H^+ resulting in the formation of $[\text{Rh}^{\text{I}}(\text{CO})(\text{PPh}_3)_3]^+$ (eqs 3 and 4):



Such a reaction sequence has been observed for other transition metal hydrides.^{11–14} After conversion to a common reference potential scale the values observed for reduction of $[\text{Rh}^{\text{I}}(\text{CO})(\text{PPh}_3)_3]^+$ are close to the published -0.88 and -1.15 V vs SCE, respectively, measured in THF¹⁵ and -1.31 and

(10) Bond, A. M.; Henderson, T. L. E.; Mann, D. R.; Mann, T. F.; Thormann, W.; Zoski, C. G. *Anal. Chem.* **1988**, *60*, 1878–1882, and references therein.

(11) Marken, F.; Bond, A. M.; Colton, R. *Inorg. Chem.* **1995**, *34*, 1705–1710.

(12) Bianchini, C.; Peruzzini, M.; Ceccanti, A.; Laschi, F.; Zanello, P. *Inorg. Chim. Acta* **1997**, *259*, 61–70.

(13) Guedes da Silva, M. F. C. *Port. Electrochim. Acta* **1996**, *14*, 31–43.

(14) Smith, K.-T.; Rømming, C.; Tilset, M. *J. Am. Chem. Soc.* **1993**, *115*, 8681–8689, and references therein.

(15) Lahuerta, P.; Soto, J.; Mugnier, Y.; Moïse, C.; Laviron, E. *New J. Chem.* **1987**, *11*, 411–414.

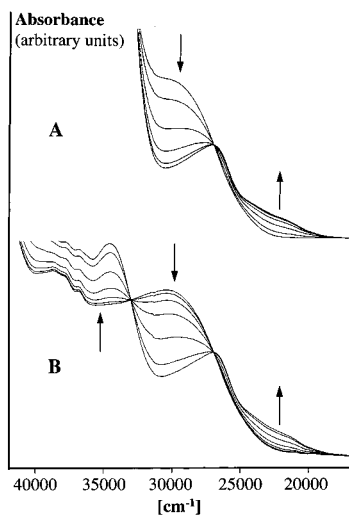


Figure 2. (A) Spectral changes accompanying electrochemical oxidation of $\text{Rh}(\text{H})(\text{CO})(\text{PPh}_3)_3$ in a dichloromethane solution at 223 K. (B) As for (A) but with 4-fold molar excess of triphenylphosphine. Arrows indicate the direction of change. Estimated values of ϵ for $\text{Rh}^{\text{I}}(\text{H})(\text{CO})(\text{PPh}_3)_3$ are $3.6 \times 10^4 \text{ M}^{-1} \text{ cm}^{-1}$ ($\lambda = 34\,500 \text{ cm}^{-1}$), $1.8 \times 10^4 \text{ M}^{-1} \text{ cm}^{-1}$ ($\lambda = 26\,500 \text{ cm}^{-1}$); and for $[\text{Rh}^{\text{II}}(\text{H})(\text{CO})(\text{PPh}_3)_3]^+$ is $2.7 \times 10^4 \text{ M}^{-1} \text{ cm}^{-1}$ ($\lambda = 30\,500 \text{ cm}^{-1}$).

-1.56 vs Ag/Ag^+ , respectively, measured in CH_3CN .¹⁶ The second oxidation process observed in voltammetric studies in acetonitrile^{5,6} is complicated by interaction with the solvent.

The $[\text{Rh}^{\text{II}}(\text{H})(\text{CO})(\text{PPh}_3)_3]^+$ cation was initially electrogenerated under a nitrogen atmosphere in situ in a platinum OTTLE cell at a potential which was 250 mV more positive than the reversible potential of the first oxidation process. The OTTLE experiments were carried out at low temperature (210 K) in order to achieve complete chemical stability on the synthetic time scale of the product of the first oxidation process of the bulk electrolysis. Electrooxidation was performed both with and without triphenylphosphine present in the solution to give the electronic spectra reported in Figure 2 (parts A and B, respectively). Triphenylphosphine, when present in a 4-fold excess (Figure 2A), obscures the far UV region of the spectrum, but otherwise both experiments give identical results. The well-defined isosbestic points are consistent with the reaction given in eq 2 being valid on the synthetic time scale at low temperature and in the absence of oxygen. In bulk electrooxidation experiments conducted on the hour time scale at 20 °C, slow decomposition of $[\text{Rh}^{\text{II}}(\text{H})(\text{CO})(\text{PPh}_3)_3]^+$ occurs to give $[\text{Rh}^{\text{I}}(\text{CO})(\text{PPh}_3)_3]^+$ as identified by IR measurements^{3,8,16} and comparison of data obtained from an authentic sample of $[\text{Rh}^{\text{I}}(\text{CO})(\text{PPh}_3)_3]\text{BF}_4$. IR carbonyl bands are 1917 cm^{-1} for $\text{Rh}^{\text{I}}(\text{H})(\text{CO})(\text{PPh}_3)_3$ and 1977 cm^{-1} for $[\text{Rh}^{\text{I}}(\text{CO})(\text{PPh}_3)_3]^+$ in dichloromethane solution. Small quantities of other unidentified product(s) may be related to those formed by reaction of the hydride complex with adventitious oxygen.¹⁷

NMR and EPR Spectroscopy. The $[\text{Rh}^{\text{II}}(\text{H})(\text{CO})(\text{PPh}_3)_3]^+$ cation also was electrogenerated for proton NMR and EPR measurements using the same applied potential in the OTTLE experiments but with a platinum basket working electrode. The electrogeneration was carried out at both low (ca. 210 K) and ambient temperature, and this had no effect the EPR spectrum of the product. Coulometric monitoring of this oxidation process is consistent with a one electron process, and comparison of voltammograms before and after bulk electrolysis confirms the

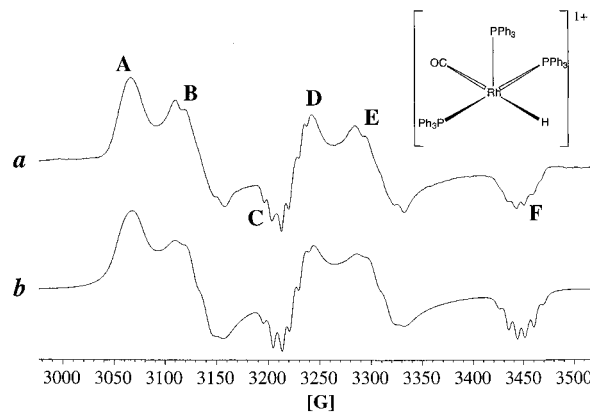


Figure 3. (A) Experimental EPR spectrum (Bruker Instrument) of the electrogenerated $[\text{Rh}^{\text{II}}(\text{H})(\text{CO})(\text{PPh}_3)_3]^+$ complex at 77 K and (B) simulated spectrum.

complete chemical and electrochemical reversibility of the first oxidation process.

At 20 °C, the ^1H NMR signal¹⁸ resulting from the hydridic proton of the $\text{Rh}(\text{H})(\text{CO})(\text{PPh}_3)_3$ was observed before electrolysis as a singlet at ca. -9.8 ppm . The fine structure expected from coupling to rhodium and phosphorus cannot be resolved at ambient temperature.¹⁸ ^1H NMR spectra of the hydride resonance obtained from solutions containing different ratios of the Rh(I) and Rh(II) species were recorded during the course of oxidative electrolysis. Substantial broadening of the signal was observed for electrolyzed samples containing ca. 10 and 20% of the oxidized form, and the signal completely disappeared for solutions containing greater than 40% of the Rh(II) complex. This result confirms that $[\text{Rh}^{\text{II}}(\text{H})(\text{CO})(\text{PPh}_3)_3]^+$ is a paramagnetic 17 electron system and that the electron self-exchange reaction between the $\text{Rh}^{\text{I}}(\text{H})(\text{CO})(\text{PPh}_3)_3$ and $[\text{Rh}^{\text{II}}(\text{H})(\text{CO})(\text{PPh}_3)_3]^+$ complexes is very fast. A fast electron self-exchange process also is consistent with the reversible diffusion controlled process observed in cyclic and rotating disk voltammetric experiments.

An EPR spectrum of the electrochemically generated cationic $[\text{Rh}^{\text{II}}(\text{H})(\text{CO})(\text{PPh}_3)_3]^+$ species in frozen dichloromethane (0.2 M $[\text{Bu}^n_4\text{N}]\text{BF}_4$ solution (77 K)) is presented in Figure 3a. The complex signal consists of several lines, which indicates strong anisotropy of the g -value and the presence of hyperfine structure. The signal manifold comprises two similar sets of lines (A, B, C and D, E, F), each set corresponding to a significant anisotropy of the g -value. However, the C and D lines partly overlap. Splitting between the two sets of lines is caused by strong hyperfine interaction of the unpaired electron in a low spin Rh(II) complex with a nucleus, possessing the nuclear spin of 1/2. Further hyperfine splitting can be discerned in the components C and F.

If the original trigonal bipyramidal structure¹⁹ (C_{3v} symmetry) were retained for the cationic species $[\text{Rh}^{\text{II}}(\text{H})(\text{CO})(\text{PPh}_3)_3]^+$, one would expect to observe a uniaxial EPR signal showing only two g -values. However the three g -values observed imply lowering of the symmetry upon oxidation. Indeed, the trigonal bipyramidal Rh(II) complex would be Jahn–Teller unstable and may rearrange by widening the P–Rh–P angle^{20,21} which would

(17) Dudley, C. W.; Read, G.; Walker, P. J. C. *J. Chem. Soc., Dalton Trans.* **1974**, 1926–1931.

(18) Dewhurst, K. C.; Keim, W.; Reilly, C. A. *Inorg. Chem.* **1968**, *7*, 546–551.

(19) La Placa, S. J.; Ibers, J. A. *Acta Crystallogr.* **1965**, *18*, 511–519.

(20) Jean, Y.; Eisenstein, O. *Polyhedron* **1988**, *7*, 405–407.

(21) Reihl, J.-F.; Jean, Y.; Eisenstein, O.; Pélissier, M. *Organometallics* **1992**, *11*, 729–737.

(16) Zotti, G.; Zecchin, S.; Pilloni, G. *J. Organomet. Chem.* **1983**, *246*, 61–71.

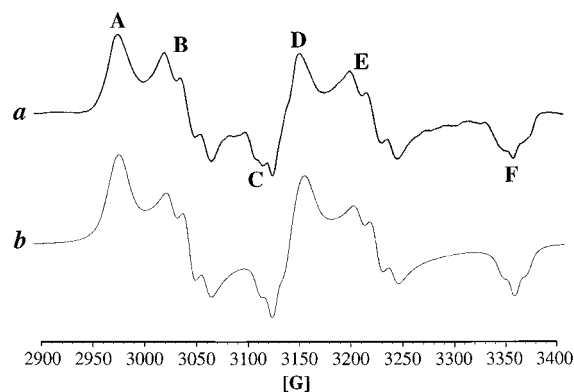


Figure 4. (A) Experimental EPR spectrum (Varian Instrument) of the electrogenerated $[\text{Rh}^{\text{II}}(\text{D})(\text{CO})(\text{PPh}_3)_3]^+$ complex at 77 K and (B) simulated spectrum.

result in a square pyramidal structure (C_s symmetry, see Figure 3). This rearrangement may occur virtually without an activation barrier, and, therefore, the proposal of a structural rearrangement is not inconsistent with the fast homogeneous and heterogeneous electron-transfer rates suggested by voltammetric and NMR data, respectively. Crystallographic studies also provide examples of pentacoordinate Rh(II) complexes having near square pyramidal geometry.^{22,23}

A square pyramidal structure with a phosphorus atom at the apex would account for the anisotropy of the g -value. The splitting between the two sets of lines (A, B, C and D, E, F) appears to be due to the hyperfine coupling with the apical phosphorus, which is amplified by the mixing of the singly occupied d_z^2 rhodium orbital and the apical phosphorus s -orbital. The hyperfine structure of the components C and F must be due to the equatorial phosphorus nuclei, the proton and the central rhodium atom, all of which have a spin of 1/2.

Computer simulation of the EPR spectrum using the Bruker "Simfonia" program was undertaken in order to confirm both the above interpretation of the spectrum and to quantify the values of the EPR parameters. Figure 3b presents the result of the simulation with the following parameters: $g_1 = 2.1155$, $g_2 = 2.0690$, $g_3 = 2.0010$; $A(\text{P}_{\text{ap}})_1 = 175.0 \text{ G}$ ($172.83 \times 10^{-4} \text{ cm}^{-1}$); $A(\text{P}_{\text{ap}})_2 = 176.0 \text{ G}$ ($170.00 \times 10^{-4} \text{ cm}^{-1}$), $A(\text{P}_{\text{ap}})_3 = 230.0 \text{ G}$ ($214.85 \times 10^{-4} \text{ cm}^{-1}$) (one nucleus); $A(\text{eq})_1 = 4.0 \text{ G}$ ($3.96 \times 10^{-4} \text{ cm}^{-1}$), $A(\text{eq})_2 = 13.0 \text{ G}$ ($12.57 \times 10^{-4} \text{ cm}^{-1}$), $A(\text{eq})_3 = 9.4 \text{ G}$ ($8.79 \times 10^{-4} \text{ cm}^{-1}$) (three nuclei: two P and one H); $A(\text{Rh})_1 = 12.0 \text{ G}$ ($11.87 \times 10^{-4} \text{ cm}^{-1}$); $A(\text{Rh})_2 = 4.0 \text{ G}$ ($3.87 \times 10^{-4} \text{ cm}^{-1}$); $A(\text{Rh})_3 = 16.5 \text{ G}$ ($15.44 \times 10^{-4} \text{ cm}^{-1}$) (one nucleus); line widths for 1, 2, and 3 components are 11.0, 9.0, and 4.0 G, respectively. A Gaussian line shape was used in the simulation, and the comparison with experiment is excellent.

An EPR spectrum of the species prepared chemically by ferricenium oxidation represents the superposition of the above spectrum and that of the residual ferricenium cation.

The experimental and simulated spectra of the deuterated Rh(II) compound, $[\text{Rh}^{\text{II}}(\text{D})(\text{CO})(\text{PPh}_3)_3]^+$, are shown in Figure 4

(22) Connelly, N. G.; Emslie, D. J. H.; Metz, B.; Orpen, A. G.; Quayle, M. J. *J. Chem. Soc., Chem. Commun.* **1996**, 2289–2290.

(23) Peng, S.-M.; Peters, K.; Peters, E.-M.; Simon, A. *Inorg. Chim. Acta* **1985**, 101, L35-L36.

and results confirm the assignment of parameters associated with the ^1H nucleus. The simulation of the deuteride analogue was undertaken with the same g -values as for the hydride and the following hyperfine coupling constants: $A(\text{P}_{\text{ap}})_1 = 180.0 \text{ G}$ ($177.77 \times 10^{-4} \text{ cm}^{-1}$); $A(\text{P}_{\text{ap}})_2 = 182.0 \text{ G}$ ($175.79 \times 10^{-4} \text{ cm}^{-1}$), $A(\text{P}_{\text{ap}})_3 = 235.0 \text{ G}$ ($219.53 \times 10^{-4} \text{ cm}^{-1}$) (one nucleus); $A(\text{P}_{\text{eq}})_1 = 6.0 \text{ G}$ ($5.93 \times 10^{-4} \text{ cm}^{-1}$), $A(\text{P}_{\text{eq}})_2 = 16.0 \text{ G}$ ($15.45 \times 10^{-4} \text{ cm}^{-1}$), $A(\text{P}_{\text{eq}})_3 = 12.0 \text{ G}$ ($11.21 \times 10^{-4} \text{ cm}^{-1}$) (two nuclei); $A(\text{D})_1 = 0.6 \text{ G}$ ($0.59 \times 10^{-4} \text{ cm}^{-1}$); $A(\text{D})_2 = 1.96 \text{ G}$ ($1.89 \times 10^{-4} \text{ cm}^{-1}$), $A(\text{D})_3 = 1.38 \text{ G}$ ($1.29 \times 10^{-4} \text{ cm}^{-1}$) (one nucleus); $A(\text{Rh})_1 = 8.0 \text{ G}$ ($7.90 \times 10^{-4} \text{ cm}^{-1}$); $A(\text{Rh})_2 = 3.0 \text{ G}$ ($2.90 \times 10^{-4} \text{ cm}^{-1}$); $A(\text{Rh})_3 = 4.0 \text{ G}$ ($3.74 \times 10^{-4} \text{ cm}^{-1}$) (one nucleus); line widths for 1, 2, and 3 components are 9.0, 8.0, and 6.0 G, respectively. Differences between the rhodium hyperfine coupling constants in the protonated and deuterated species are not regarded as being statistically reliable.

Finally, it can be noted that the g -values and $A(\text{Rh})$ are comparable with those published for other compounds^{22,24,25} which further supports the assignment of the EPR parameters for the $[\text{Rh}^{\text{II}}(\text{H})(\text{CO})(\text{PPh}_3)_3]^+$ complex.

Conclusions

Electrochemical oxidation of the widely used 18 electron rhodium(I) catalyst $\text{Rh}^{\text{I}}(\text{H})(\text{CO})(\text{PPh}_3)_3$ leads to an unusually stable monomeric 17 electron rhodium(II) complex $[\text{Rh}^{\text{II}}(\text{H})(\text{CO})(\text{PPh}_3)_3]^+$. The oxidation is so facile that it may need to be considered in processes catalyzed by $\text{Rh}^{\text{I}}(\text{H})(\text{CO})(\text{PPh}_3)_3$. Voltammetric and UV–visible spectral monitoring of the oxidation process in the presence and absence of PPh_3 ligand confirm that the five-coordinate geometry is thermodynamically favored in both oxidation states at low temperatures in dichloromethane. The EPR study of the electrochemically generated cation reveals an uncommonly rich spectrum and, in concert with other techniques, indicates that a rapid rearrangement from trigonal bipyramidal to square pyramidal structure occurs upon oxidation. Commonly, monomeric rhodium redox chemistry is dominated by the Rh(I) and Rh(III) oxidation states and reductive elimination and oxidative addition reactions. Many of the stable complexes of formally divalent rhodium are in fact metal–metal bonded, dimeric, diamagnetic compounds.²⁶ The identification of a stable 17 electron monomeric Rh(II) paramagnetic compound therefore establishes another novel feature of this well-known catalytic system where even number diamagnetic 18 or 16 electron species are known to be important. Further oxidation of $[\text{Rh}^{\text{II}}(\text{H})(\text{CO})(\text{PPh}_3)_3]^+$ leads to the transient formation of $[\text{Rh}^{\text{III}}(\text{H})(\text{CO})(\text{PPh}_3)_3]^{2+}$ which undergoes a reductive elimination reaction to form the well-known $[\text{Rh}^{\text{I}}(\text{CO})(\text{PPh}_3)_3]^+$ complex.

Acknowledgment. The authors wish to thank Dr. Graham Heath, Research School of Chemistry, The Australian National University, Canberra for the use of UV/vis Spectroelectrochemical facilities. This paper is dedicated to the memory of Dr. Scott A. Olsen, who died (aged 29) on April 29, 1996.

JA973164X

(24) Anderson, J. E.; Gregory, T. P. *Inorg. Chem.* **1989**, 28, 3905–3909.

(25) Rotov, A. V.; Zhilyaev, A. N.; Baranovskii, I. B.; Larin, G. M. *Russ. J. Inorg. Chem.* **1989**, 34, 1079–1081.

(26) See, for example: Cotton, F. A.; Walton, R. A. *Multiple Bonds between Metal Atoms*, 2nd ed.; Clarendon Press: Oxford, 1993.